International Immunopharmacology 22 (2014) 167–175

Contents lists available at ScienceDirect

International Immunopharmacology

journal homepage: www.elsevier.com/locate/intimp

Suicide plus immune gene therapy prevents post-surgical local relapse and increases overall survival in an aggressive mouse melanoma setting

Marcela S. Villaverde [a], Kristell Combe [b], Adriana G. Duchene [c], Ming X. Wei [b], Gerardo C. Glikin [a], Liliana M.E. Finocchiaro [a,*]

[a] Unidad de Transferencia Genética, Instituto de Oncología "Ángel H. Roffo", Universidad de Buenos Aires, Argentina
[b] Cellvax Laboratoires, École Nationale Vétérinaire d'Alfort, France
[c] Facultad de Ciencias Veterinarias, Universidad de Buenos Aires, Argentina

ARTICLE INFO

Article history:
Received 3 March 2014
Received in revised form 30 May 2014
Accepted 10 June 2014
Available online 25 June 2014

Keywords:
IL-2
GM-CSF
HSV-TK
Melanoma vaccine
DMRIE
PET scan

ABSTRACT

In an aggressive B16-F10 murine melanoma model, we evaluated the effectiveness and antitumor mechanisms triggered by a surgery adjuvant treatment that combined a local suicide gene therapy (SG) with a subcutaneous genetic vaccine (Vx) composed of B16-F10 cell extracts and lipoplexes carrying the genes of human interleukin-2 and murine granulocyte and macrophage colony stimulating factor. Pre-surgical SG treatment, neither alone nor combined with Vx was able to slow down the fast evolution of this tumor. After surgery, both SG and SG + Vx treatments, significantly prevented (in 50% of mice) or delayed (in the remaining 50%) post-surgical recurrence, as well as significantly prolonged recurrence-free (SG and SG + Vx) and overall median survival (SG + Vx). The treatment induced the generation of a pseudocapsule wrapping and separating the tumor from surrounding host tissue. Both, SG and the subcutaneous Vx, induced this envelope that was absent in the control group. On the other hand, PET scan imaging of the SG + Vx group suggested the development of an effective systemic immunostimulation that enhanced ^{18}FDG accrual in the thymus, spleen and vertebral column. When combined with surgery, direct intralesional injection of suicide gene plus distal subcutaneous genetic vaccine displayed efficacy and systemic antitumor immune response without host toxicity. This suggests the potential value of the assayed approach for clinical purposes.

1. Introduction

Human malignant melanoma is an aggressive skin cancer with increasing incidence and highly resistant to conventional therapies [1]. New emerging drugs like BRAF kinase inhibitors vemurafenib and dabrafenib [2,3], the MEK inhibitor trametinib [3] and the immunostimulatory human antibody against cytotoxic T-lymphocyte antigen-4 ipilimumab [4] were recently approved. However, these drugs were able to significantly increase disease-free or overall survival only in a limited subset of melanoma patients, while presenting a high rate of adverse events. In this scenario the research on new treatments is warranted.

Besides, canine spontaneous malignant melanoma is a highly aggressive tumor too invasive to be cured only by surgical resection and frequently resistant to current therapies [5,6]. Working on this disease, we demonstrated the safety and efficacy of a surgery adjuvant approach that combines local suicide gene (SG) therapy (lipoplexes carrying the herpes simplex thymidine kinase gene – HSV*tk* – and ganciclovir) with a subcutaneous vaccine composed of tumor cell extracts and xenogeneic cells producing human interleukin-2 and granulocyte–macrophage colony-stimulating factor. After 9 years of follow-up, this open label controlled study demonstrated that this surgery adjuvant treatment was able not only to control tumor growth but also to delay or to prevent postsurgical recurrence and the outgrowth of metastases [7,8]. Furthermore, it significantly increased disease-free and overall survival while maintained the quality of life as compared to surgery only treated controls. However, the high rate of highly aggressive tumors (from 22% to 31% of the cases) in our canine melanoma trials [7–9] was the main problem that has hindered long-term control and substantially shortened veterinary patients' median overall survival. In addition, we found an underlying multicellular resistance mechanism due to the rapid cell repopulation (re-growth) of these aggressive tumors after SG treatment [10]. To get a deeper insight on the response of extremely malignant tumors to our combined treatment, we established a highly aggressive melanoma murine model by intradermal inoculation of 3×10^6 B16-F10 syngeneic cells in C57BL/6 mice.

Here we evaluated the efficacy and various effects triggered by a surgery adjuvant treatment that combined local suicide gene therapy

* Corresponding author at: Unidad de Transferencia Genética, Instituto de Oncología "A. H. Roffo" — UBA, Av. San Martín 5481, 1417 Buenos Aires, Argentina. Tel./fax: +54 11 4580 2813.
E-mail address: gglikin@bg.fcen.uba.ar (L.M.E. Finocchiaro).

http://dx.doi.org/10.1016/j.intimp.2014.06.021
1567-5769/

with a distant subcutaneous genetic vaccine, in an aggressive murine melanoma setting.

2. Materials and methods

2.1. Cell culture and extract preparation

B16-F10 murine melanoma cells (ATCC #: CRL-6475) were cultured following the supplier's indications. Sub-confluent monolayers were harvested, washed with 10 volumes of PBS and homogenized with 5 volumes of 4% (w/v) formaldehyde in PBS in a Dounce homogenizer. Homogenate pellets were washed 3 times with 5 volumes of PBS and resuspended in the same volume before injection.

2.2. Plasmids

Plasmids psCMVβgal, psCMVhIL2 and psCMVmGMCSF were built by replacing the HSV thymidine kinase gene of psCMVtk [7] by *Escherichia coli* β-galactosidase, human IL-2 and mouse GM-CSF genes respectively. While human IL-2 is active on immune mouse cells, human GM-CSF is not, and the specific cytokine is required. Plasmids were amplified in *E. coli* DH5α (Invitrogen, Carlsbad, CA, USA), grown in LB medium containing 100 mg/ml neomycin and purified by ion exchange chromatography (Qiagen, Valencia, CA, USA).

2.3. Liposome preparation and in vivo lipofection

DMRIE (1,2-dimyristyl oxypropyl-3-dimethyl-hydroxyethyl-ammonium bromide) was synthesized and provided by BioSidus SA (Buenos Aires, Argentina). DOPE (1,2-dioleoyl-sn-glycero-3-phosphatidyl ethanolamine) was from Sigma-Aldrich (St Louis, MO, USA). Liposomes were prepared by sonication of equimolar amounts of DMRIE and DOPE [7]. Before injection, liposomes and plasmid DNA (1:2 v:v) were mixed and allowed to combine at room temperature for 10 min. Then ganciclovir (GCV: 625 μg) and B16-F10 cell extracts were added as described below.

2.4. Murine tumor model and in vivo gene transfer

C57BL/6 mice (17–20 g body weight, 6–8 weeks old females) were purchased at Harlan Laboratories® (Gannat, France). Three million B16-F10 cells were intradermally injected in the left leg of C57BL/6 mice. Tumor growth was daily monitored with a caliper. Tumor volumes were calculated using the formula $a^2 \times b / 2$ ("a": shortest diameter; "b": longest diameter). When reaching about 250 mm^3 tumors were intratumorally injected with 50 μl of lipoplexes carrying psCMVβgal plus GCV (control βg) or psCMVtk plus GCV (SG) twice a week. When indicated, intratumoral treatments were combined with subcutaneous injection of whole B16-F10 cell extract (10 μl) plus lipoplexes containing psCMVhIL2 and psCMVmGMCSF (Vx, 60 μl). Primary B16-F10 tumors were surgically excised (under anesthesia) when tumor volume reached approximately 1500 mm^3 (between 3 and 13 days after B16-F10 cell injection). After surgery, tumor beds were injected with 100 μl (25 μl in 4 different places) of the appropriate lipoplexes accordingly to each group. Initial treatment conditions were re-established one week after surgery. Local relapse was daily monitored. Mice were humanely euthanized when recurrent tumors reached a volume of about 2000 mm^3. Non-relapsing mice were euthanized on day 50 after the initiation of the treatment. The care and housing of animals followed the institutional guidelines of L'École Nationale Vétérinaire d'Alfort (ENVA, France), under the supervision of authorized staff.

2.5. Immune-histochemical analysis of tumors

The resected tumors were fixed in 10% buffered formalin and embedded in paraffin. Paraffin-embedded sections (5 μm) were blocked with 10% bovine serum albumin (BSA, Sigma-Aldrich) in PBS for 1 h. Then, they were incubated with anti-CD4 (M7310, 1:80; DAKO, Les Ulis, France), anti-CD8 (M7103, 1:100; DAKO), anti-monocyte (MAC387, 1:100; Serotec, NC; USA), anti-CD11b (M1/70, 1:100; Ebioscience, CA, USA), anti-FoxP3 (14-5773-82, 1:500; Ebioscience), and anti-GR1 (RB6-8C5, 1:100; Ebioscience) in PBS overnight. Sections were washed and incubated with Alkaline phosphatase-conjugated secondary antibody (1:1000; Santa Cruz, TX, USA) for 2 h and then incubated with NBT/BCIP in Tris buffer (pH 9.5) for 2 h. Besides, tumor sections were stained with hematoxylin and eosin (H&E) for histopathological analysis.

2.6. Micro-positron emission tomography (micro-PET)

Positron emission tomography (PET) scan imaging of treated mice was carried out at the Nuclear Medicine Service of Tenon Hospital (Paris, France). Mice were anesthetized by isoflurane (DDG 923) inhalation and injected in the retro-orbital sinus with 6 ± 1 MBq of ^{18}F-fluorodeoxyglucose (^{18}F-FDG). Image acquisition was performed for 10 min, 1 h after tracer injection, with the Mosaic® small animal PET scanner (Philips Medical Systems, OH, USA).

2.7. Toxicity

During treatment all animals were monitored for changes in attitude, body temperature, body weight, skin, and mortality. After gross necropsy and histopathology observation for toxicity, principal organs were removed and fixed by 4% neutral formaldehyde at room temperature for 48 h. The paraffin-embedded sections (5 μm) were H&E stained for histopathological analysis.

2.8. Statistical analysis

Local disease-free and overall median survivals were calculated by Kaplan–Meier analysis and curves were compared by Log-rank test by using GraphPad Prism® 5.00 software (GraphPad Software, La Jolla, CA, USA). Differences in pseudocapsule formation and enlarged thymus incidence values were compared by two tailed Fisher's Exact test.

3. Results and discussion

3.1. Fast growing B16-F10 melanoma tumors were resistant to treatment

To get a deeper insight on the highly malignant tumor response to our local suicide gene (SG) plus a subcutaneous genetic vaccine (Vx) combined treatment, we established a highly aggressive melanoma murine model by intradermal inoculation of 3×10^6 B16-F10 syngeneic cells in C57BL/6 mice.

Treatment was individualized, each animal being considered as a single case. A CONSORT-like flow chart [11] of the treatment is depicted in Fig. 1. When tumor volume was about 250 mm^3, animals were treated either with βgal + ganciclovir (βg) or HSV*tk* + ganciclovir suicide gene (SG) intratumor lipoplex treatment twice a week. Half of the mice of each group (βg + Vx and SG + Vx respectively) also received the subcutaneous Vx containing whole B16-F10 cell formolized extracts and lipoplexes carrying the genes of human interleukin-2 (hIL-2) and murine granulocyte–macrophage colony-stimulating factor (GM-CSF). The growth of these aggressive murine melanoma was heterogeneous, paralleling that of canine melanomas [7,9]. However, in the Vx treated groups (βg + Vx and SG + Vx), tumor growth appeared to be less scattered (Fig. 2a).

Consistently with our results in highly aggressive canine melanomas [7–9], pre-surgical SG treatment neither alone nor combined with Vx was able to slow down the fast in situ progression of this aggressive B16-F10 murine melanoma (Fig. 2a). Mean tumor growth rate was

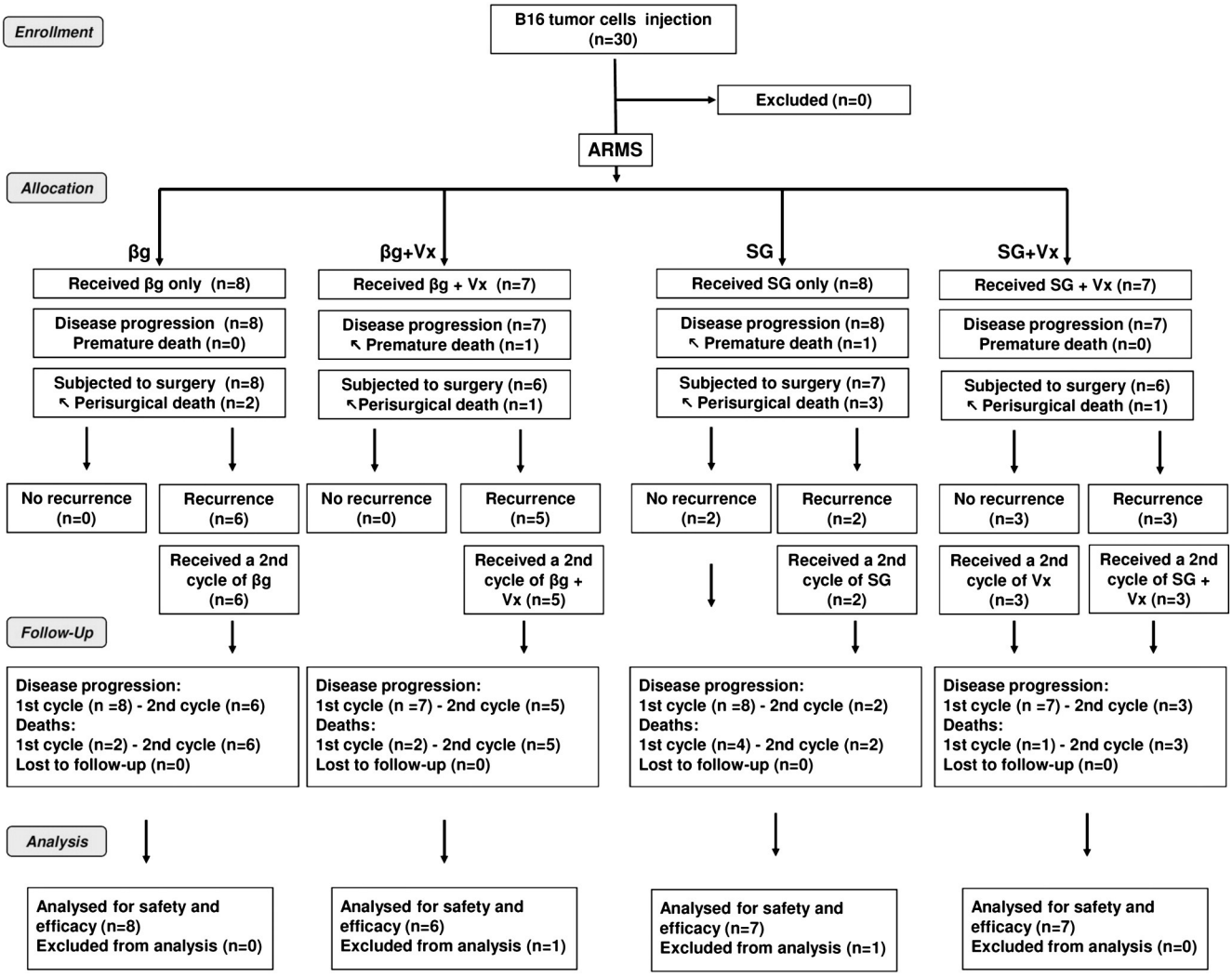

Fig. 1. CONSORT-like flow chart of the treatment.

not significantly different between SG treated groups (SG and SG + Vx) and the control (βg) group (Fig. 3a).

A more efficient version of both SG and the gene transfer vector would be useful to improve local tumor control. Since our plasmid carries the wild type HSVtk-1 SG, the local outcome could be enhanced by using a splice corrected version of the gene [12], a mutant like SR39 [13] or the novel TK.007 [14]. On the other hand, an emerging nonviral nanoparticle mediated gene transfer could be as effective as adenoviral vectors [15]. Efficient adenoviral vectors were frequently used [16], even keeping its intrinsic oncolytic activity [17]. However, because of anti-viral immunological reactions and other unwanted toxic interactions, current adenoviral-based clinical applications are strictly limited to in situ administration against primary tumors [18]. Therefore these viral vectors would not be useful in our treatment scheme.

Surprisingly, we observed that the subcutaneous vaccine (βg + Vx group) significantly increased the mean tumor growth rate ($p < 0.0001$ with respect to the other three groups, Fig. 3a). These results suggest a paradoxical increase of tumor size attributable to treatment effects rather than early tumor progression, as it happened in our canine patients [7–9]. This pseudo-progression could be the result of a vaccination induced inflammatory response [19] that was not compensated by the effects of the suicide gene on tumor cells.

3.2. Suicide gene system delayed or prevented post-surgical local tumor relapse

All tumors were removed by surgery at a tumor volume of about 1500–2000 mm^3. The surgical margin of the cavity was injected with lipoplexes carrying the respective βg or SG genes and initial treatment conditions were re-established one week post-surgery.

All post-surgical surviving mice of βg and βg + Vx groups displayed local tumor relapse. However, a recurrence delay was observed in 1 (of 6) βg, and in 1 (of 5) βg + Vx treated animals. In the latest case the tumor growth rate was diminished. Conversely, both post-surgical SG and SG + Vx treatments, significantly prevented (in 50% of mice) or delayed (in the remaining 50%) post-surgical recurrence (Fig. 2b).

Taken as a whole, the post-surgical mean growth rate in all the groups was significantly lower than that of the respective primary tumors ($p < 0.0001$ in βg + Vx, SG and SG + Vx groups; and $p < 0.03$ in βg groups) (Fig. 3a,b). Furthermore mean growth rates of SG and SG + Vx relapsing tumors were significantly lower than those of βg and βg + Vx primary tumors (Fig. 3b, $p < 0.0001$).

It is worth to note the remarkable reduction of the mean tumor growth rate of βg + Vx group after surgery, that not only was under that of its own primary tumors ($p < 0.0001$) but also dropped below that of βg relapsing tumors (Fig. 3a,b).

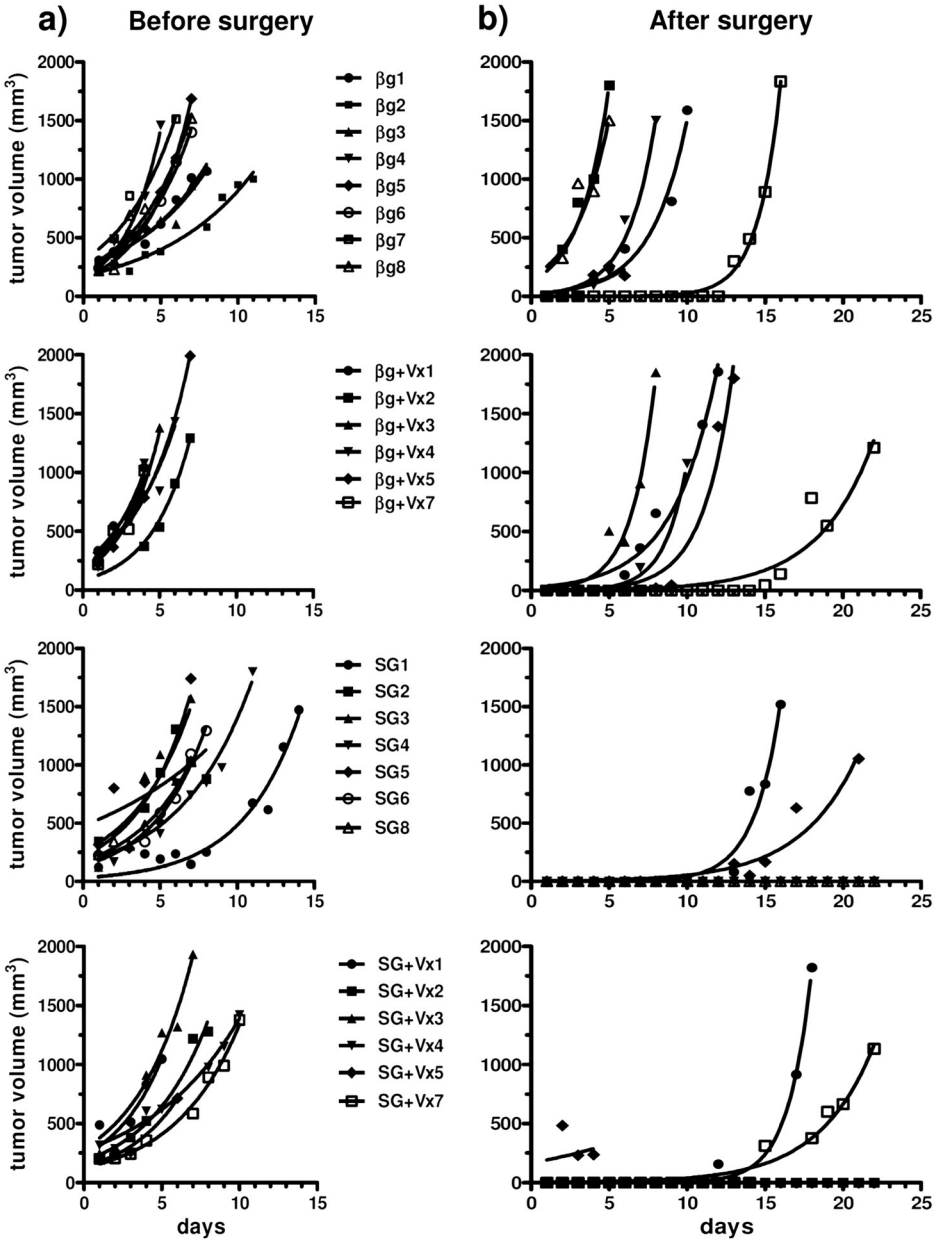

Fig. 2. Individual tumor responses to treatments before (a) and after (b) surgery. 3×10^6 B16-F10 cells were intradermally injected in the left hind legs of C57BL/6 mice ($n = 6–8$). Tumor volumes were measured daily as described in Materials and methods. Individual tumor growth was analyzed by exponential growth equation. Individually identified mice were followed over the treatment until death. βg: β-galactosidase; Vx: genetic vaccine; SG: suicide gene.

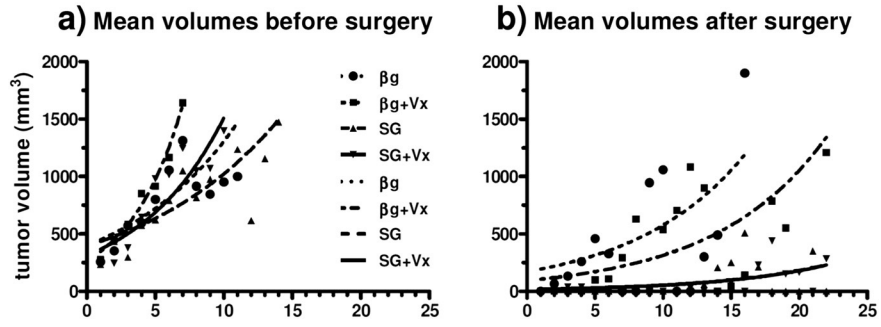

Fig. 3. Means of individual responses to treatments before (a) and after (b) surgery displayed in Fig. 2. Data were plotted separately at the same time scale for the sake of visual simplicity. Differences between curves were analyzed by exponential growth equation and curves were compared by Extra sum-of-square F test. Before surgery: $p < 0.0001$ βg + Vx vs. all others. After surgery: $p < 0.02$ βg vs. βg + Vx; $p < 0.0001$ βg vs. SG and SG + Vx; $p < 0.0001$ βg + Vx vs. SG and SG + Vx. Before and after surgery: $p < 0.0001$ primary vs. recurrent tumors in βg + Vx, SG and SG + Vx; $p < 0.03$ primary vs. recurrent tumors in βg. βg: β-galactosidase; Vx: genetic vaccine; SG: suicide gene.

3.3. The combined treatment significantly prolonged tumor-free and overall survival

Kaplan–Meier tumor-free survival curves (Fig. 4a,c) showed that βg and βg + Vx-treated groups displayed a median local tumor relapse at 4 and 7 days respectively, whereas SG and SG + Vx treated groups displayed significantly increased tumor-free survivals up to 32 days (respective ranges 13–50 and 2–50).

The Kaplan–Meier median overall survival of the SG + Vx group (38.5 days, range 5–50) significantly increased ($p < 0.04$ and $p < 0.02$) with respect to βg (15 days, range 9–23) and βg + Vx (17 days, range 8–30) (Fig. 3b,c). Conversely, even though the median overall survival of SG was 31 days (range 8–50), its survival curve was not significantly different from those of βg and βg + Vx.

3.4. Both the subcutaneous vaccine and the suicide gene induced the formation of a pseudocapsule

Surgically excised tumors were enveloped by a pseudocapsule probably promoted by the local immune response, given that both SG and the Vx induced this envelope that was completely absent in βg treated tumors. The subcutaneous Vx generated this tumor wrapping in 67% and 83% of the βg + Vx and SG + Vx groups ($p < 0.015$ and 0.003 respectively compared to the βg group). In addition, repeated intratumor injections of SG, by killing cells in an "immunogenic fashion", induced this tumor pseudocapsule in 57% of SG mice ($p < 0.026$ compared to the βg group). Consistent with our hypothesis, Mac Keon et al. [20] found a pseudocapsule at the vaccination site with dendritic cells. Along this line, the presence of tumor pseudocapsules is known to be a favorable prognostic factor in patients with non-small lung cancer, [21], colorectal liver metastases [22,23], osteosarcoma [24] and soft tissue sarcomas [25].

3.5. Pseudocapsules appeared infiltrated by immune cells

Once mice underwent surgery, excised tumors were fixed and stained for microscopic analysis as described in the Materials and methods section. Since we established an extremely aggressive model of melanoma, in every group all primary tumors displayed a high grade of anaplasia, high mitotic index and extensive necrotic areas.

Microscopic analysis revealed a pseudocapsule separating connective and tumor tissues in all treated groups (βg + Vx, SG and SG + Vx) (Fig. 5). This fibrotic tissue pseudocapsule appeared associated with a significant immune reaction, suggesting a direct link between this structure and the local immune response. It is worth to note that the thickness of the pseudocapsule increased from no capsule for βg to the thickest for the SG + Vx group, being intermediate for βg + Vx and SG (Fig. 4). This agrees with previous reports where this pseudocapsule was observed, being more continuous, thicker and better developed in therapy responsive tumors [25,26].

A microscopically detected incomplete pseudocapsule was found only in 1 (of 8) mouse of the βg group in limited areas around the tumor, probably due to a site-specific early host-recognition antitumor immune response. Despite that cationic lipids and plasmid DNA immunostimulatory sequences might also increase local tumor immunogenicity [27,28], in the βg group this early inflammatory reaction at the site of tumorigenesis failed to reach a minimal pseudocapsular structure while the growing tumor crowded and physically invaded the surrounding tissue.

3.6. ^{18}F-FDG PET scan imaging suggested a systemic immune system reaction against melanoma

To provide in vivo evidence of local and systemic disease development as well as to monitor in vivo immune response, positron emission tomography (PET) scan imaging of treated mice was carried out.

An accumulative ^{18}F-fluorodeoxyglucose (^{18}F-FDG) image of local tumor relapse was observed in βg and βg + Vx (t arrows, Fig. 6a,b). Compared to the large and disseminated tumor of βg treated animal, the βg + Vx treated mouse showed a confined round tumor, due to a covering pseudocapsule confirmed by necropsy. In contrast, no recurrent disease, in agreement with macroscopic evaluation, was observed in the evaluated SG and SG + Vx treated mice (Fig. 6c,d). On the other hand, while one of 2 evaluated SG only treated mice showed a pulmonary metastasis confirmed by necropsy 23 days later, none of the 2 evaluated SG + Vx did so (Fig. 6c,d). It is worth to point out that the SG animal with a pulmonary metastasis lacked for a pseudocapsule enveloping the primary tumor.

Undoubtedly a highly encouraging outcome was the confirmation by PET scan imaging, of an effective immune stimulation that enhanced glucose metabolism in SG + Vx treated mice (Fig. 6d). The absence of distant disease in these animals, confirmed by necropsy 20 and 25 days later, strongly suggests that the increased accumulation of ^{18}F-FDG in the vertebral column, thymus, spleen and upper neck lymph nodes was not due to tumor metastasis but rather to the presence of active immune cells in the SG + Vx group. Previous reports

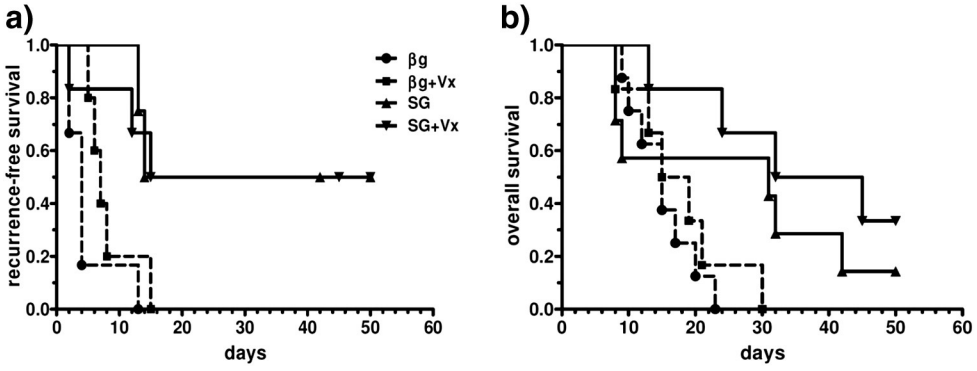

c)

MEDIAN SURVIVAL(days)	βg	βg+Vx	SG	SG+Vx	βg *vs* (p<)	
					SG	SG+Vx
Recurrence-free	4 (2-13)	7 (5-15)	>32 (13-50)	>32 (2-50)	0.02	0.05
Overall	15 (9-23)	17 (8-30)	31 (8-50)	39 (13-50)	ns	0.004

Fig. 4. Kaplan–Meier analysis of recurrence-free (a) and overall (b) survival. Data were analyzed by Kaplan–Meier log-rank test and median survival results are displayed in panel (c). βg: β-galactosidase; Vx: genetic vaccine; SG: suicide gene.

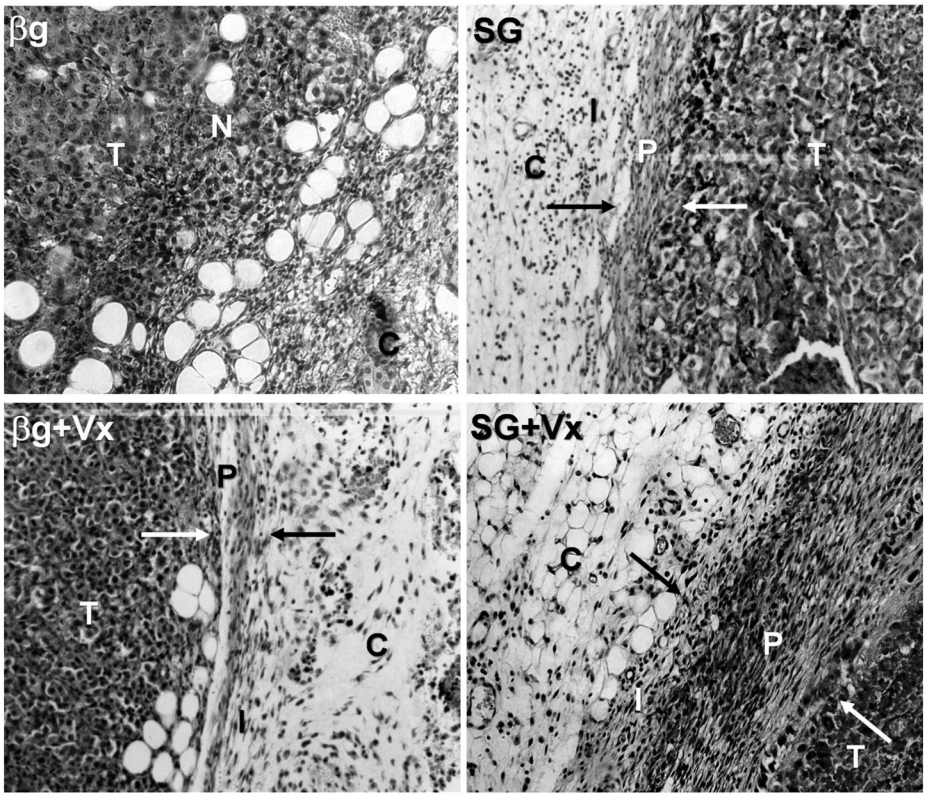

Fig. 5. Pseudocapsule histological analysis. Surgically excised primary tumors were fixed and prepared for histological analysis as described in the Materials and methods section. The photographs show representative patterns of each tumor group (black arrows indicate the pseudocapsule delimiting connective tissue whereas white arrows indicate tumor tissue limit). βg: β-galactosidase; SG: suicide gene; Vx: genetic vaccine. C: connective tissue I: immune cells; N: No capsule; P: pseudocapsule; T: viable tumor cells. The arrows point to the limits of the pseudocapsule.

described PET scan as an approach to measure both tumor and antitumor immune responses to therapies [29,30].

3.7. The combined treatment significantly increased the fraction of mice with enlarged thymus

Reinforcing PET scan-evidence of a treatment induced systemic immune response, we found enlarged thymus (102.4 ± 9.8 mg, about 3-fold more weighty than those of βg) in 5 (of 6) mice (83%, $p < 0.003$) of the SG + Vx group and in 3 (of 7) mice (43%) of the SG group (111.9 ± 22.3 mg). Conversely, none of the βg or βg + Vx mice showed bigger thymus, possible due to the early death of these groups. However, while 5 (of 6) SG + Vx and 3 (of 4) SG of post-surgery surviving mice displayed greatly enlarged thymus ($p < 0.002$ and 0.03 respectively with respect to the βg group), none of the post-surgery survivors of βg or βg + Vx mice did.

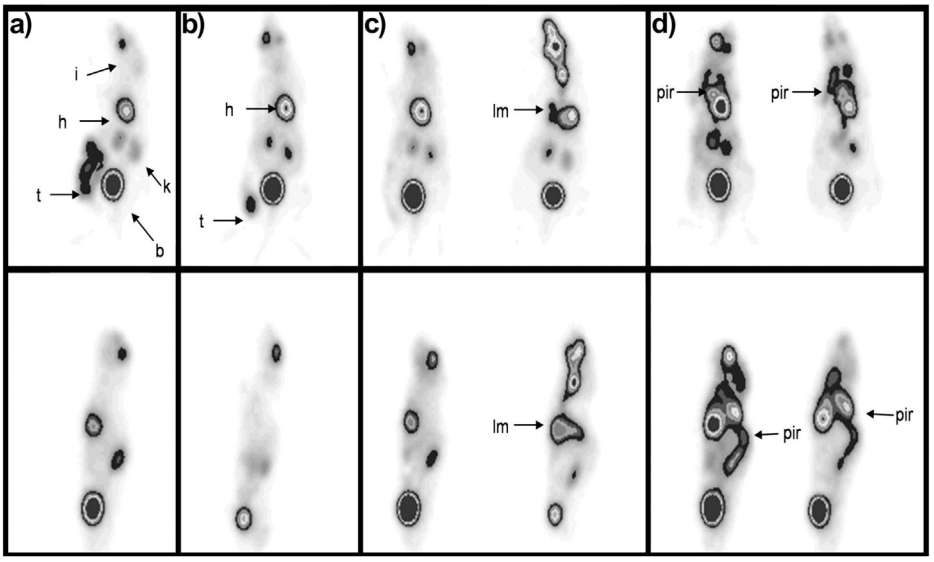

Fig. 6. ^{18}F-FDG microPET imaging of treated animals. Mice were treated as described in Materials and methods. Upper panel: coronal plane. Lower panel: sagittal plane. **(a)** βg, **(b)** βg + Vx, **(c)** SG and **(d)** SG + Vx. Arrows indicate: (i) injection site, (h) heart, (k) kidney, (t) tumor, (b), bladder, (lm) lung metastases, and (pir) possible immune response at superficial cervical lymph nodes. Number of analyzed mice: n = 1 for (a) and (b); n = 2 for (c) and (d). βg: β-galactosidase; Vx: genetic vaccine; SG: suicide gene.

3.8. Tumors were infiltrated by anti- and pro-tumorigenic immune cell populations

Infiltration by different anti/pro-tumorigenic immune cell populations was found in all surgery excised tumors [31–37] (Fig. 7).

The presence of pro-tumorigenic immune cells within defined tumor regions was demonstrated by co-localization of $Gr1^+$ and $CD11b^+$ myeloid-derived suppressor cells (MDSCs, columns 1 and 2) and $FoxP3^+$ and $CD4^+$ regulatory T cells (Tregs, columns 3 and 4) labeling images corresponding to the analogous areas of consecutive serial tumor slices [34–36] (Fig. 7). In the βg and SG groups' images, CD11b+ and Gr1+cells co-localized. It is worth to note the strong MDSC infiltrate of βg2 (second row), a fast (pre- and post-surgery) growing tumor with respect to those of βg7 (first row), the slowest post-surgery growing tumor (Figs. 2 and 7).

Even though all these fast progressing pre-surgery tumors grew regardless of the group, treatments (βg + Vx, SG and SG + Vx) seemed to decrease the number of MDSCs within tumor tissues. In addition, the better responders to the subcutaneous Vx (βg + Vx7 and SG + Vx4, upper row of each group, Figs. 2 and 7) decreased even more the amount of $CD11b^+$ cells, leaving a fraction of $Gr1^+$ cell population that did not co-localize with $CD11b^+$ labeling, indicating that most of the tumor infiltrated Gr1-labeled cells could potentially reflect other $CD11b^-$ cell populations. These data and the low pre-surgery macrophages infiltrate in those tumors that were better responders to post-surgery treatments (upper row of each group) suggest that

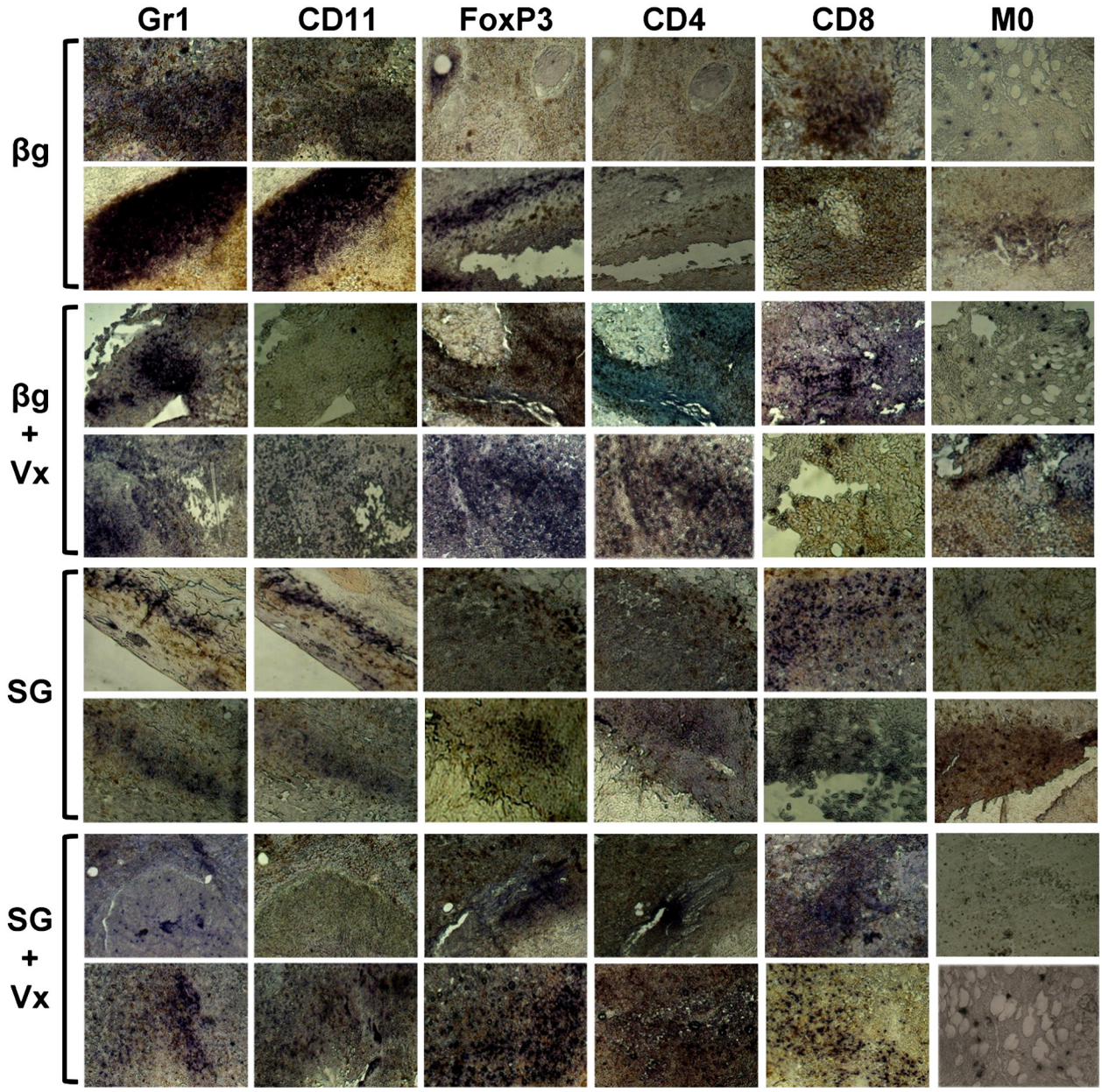

Fig. 7. Effects of treatments on tumor anti/pro-tumorigenic immune cell infiltration. Consecutive serial sections of tumors were prepared for immunohistochemical analysis with specific antibodies to identify and locate (in the same field of view): $Gr1^+$ $CD11b^+$ myeloid-derived suppressor cells (MDSCs, columns 1 and 2) and $CD4^+$ $FoxP3^+$ regulatory T cells (Tregs, columns 3 and 4). Anti-tumor cells $CD8^+$ T cells (column 5) and macrophages (column 6) were also characterized. Representative tumor sections from two different animals of each group are displayed. Each row represents a single mouse. Upper row of each group represents post-surgery (PS) treatment better response: (i) slow growing relapsed tumor (βg7 and βg + Vx7) and (ii) no relapse (SG4 and SG + Vx4). Lower row of each group represents PS treatment worse response: (i) fast growing relapsed tumor (βg2 and βg + Vx4) and (ii) relapsed tumor (SG1 and SG + Vx1). βg: β-galactosidase; Vx: genetic vaccine; SG: suicide gene.

the treatment could induce maturation and migration of these myeloid cells.

Conversely, FoxP3$^+$ staining of the nuclei of mononuclear leukocytes did not co-localize with CD4$^+$ T cells in βg, while partially co-localized and increased in all treated groups (SG, βg + Vx and SG + Vx). Recent findings suggest that FoxP3$^+$ nuclear staining may not be specific for Tregs, but can also be expressed by other activated T-cell populations [36]. In melanoma patients treated with ipilimumab, higher baseline intratumoral levels of FoxP3 were predictive of a positive clinical outcome [37]. These data, and the higher pre-surgery CD8$^+$ cells infiltrate in those tumors that were better responders to post-surgery treatments (upper row of each group), suggest that the presence of FoxP3$^+$ regulatory T cells, would be associated with positive response.

As derived from Figs. 6, and 7 and the effect of thymus enlargement, it seems likely that in our system the cytokines expression levels were high enough to induce specific antitumor immunity. Even so, an improvement of local and systemic immune control could be driven by the addition of genetic vaccine adjuvants as DAI [38].

3.9. Gene transfer treatments resulted safe

The treatment produced minor treatment-related adverse events (grade 1 o 2) following the VCOG-CTCAE criteria [39]. No treatment-related changes in attitude, body temperature and body weight were observed. The macroscopic and microscopic analyses of principal organs by histological techniques after necropsy showed no treatment-related toxicity. Kidney sections showed normal renal cortex and glomerular tufts in all groups (data not shown).

4. Conclusion

As it happened in our canine melanoma trials [7–9], present work suggests that this surgery adjuvant suicide gene (SG) and a genetic vaccination (Vx) combined therapy appears to be considerably superior to the separate monotherapies.

To achieve long-term control of highly aggressive and invasive tumors, that did not respond to pre-surgical treatments (Fig. 2a), the optimal clinical setting would be a surgery adjuvant treatment. After surgery, both SG and SG + Vx treatments, significantly prevented (in 50% of mice) or delayed (in the remaining 50%) post-surgical recurrence (Fig. 2b), as well as significantly prolonged recurrence-free and overall median survival (Fig. 4).

The basis of this combined treatment clinical efficacy was possibly due to a successful synergic interaction of local and systemic antitumor immune responses.

An interesting finding was the generation of a pseudocapsule wrapping and separating the tumor from surrounding host tissue (Fig. 5). This novel structure appeared before surgery, when tumor progression did not noticeably respond to early treatment — remodeling of the heterogeneous tumor immune infiltrating cells (Fig. 7). However, both SG and the subcutaneous Vx induced this envelope that lacked in βg treated tumors. So in agreement with previous reports [20–26], these data strongly suggest that the pseudocapsule was promoted by the local antitumor immune response induced by the treatments (βg + Vx, SG and SG + Vx) to protect the host.

This immune-generated pseudocapsule played a critical role in preventing tumor local invasion and dissemination, as corroborated by micro-positron emission tomography (PET) scan imaging. Compared to the large and disseminated unwrapped tumor of βg treated animal, the βg + Vx treated mouse showed a confined round tumor, due to a covering pseudocapsule (Fig. 6 a,b).

An extremely encouraging outcome was the PET scan images of the SG + Vx group that strongly supported the development of an effective immunostimulation that enhanced glucose metabolism in the thymus, spleen, vertebral column and upper neck lymph nodes (Fig. 6d). This trend was mimicked by the greatly enlarged weight of the thymus (about 3 times more weighty than those of βg) in 5 out of 6 SG + Vx mice.

The fact that the vaccine in the absence of suicide gene (βg + Vx group) was insufficient for inducing a meaningful systemic immune response (Fig. 6b), strongly suggests that it was boosted in its presence (Vx + SG group) (Fig. 6d).

Finally we found that the SG + Vx combined treatment, after surgical removal of the tumor, was able to elicit a powerful antitumor effect evidenced by a significant: (i) delay (in 50% of mice) or avoidance (in the remaining 50%) of post-surgical recurrence; (ii) restriction of local invasion and dissemination by inducing a pseudocapsule enclosing tumors in 83% of mice, (iii) induction of a potent local and systemic immune response as depicted in PET scan imaging, (iv) increase of the fraction of mice bearing enlarged thymus (83%); and (v) prolongation of median overall and local disease free-survival.

Conflicts of interest

M.X.W. is president and scientific director and K.C. employee of Cellvax S.A. (Evry, France). Cellvax is a service provider company (CRO). None of the vectors or treatment procedures used in the present work is property of Cellvax. No other potential conflicts of interest should be disclosed.

Acknowledgments

We thank Dr. Norberto D. Judewicz for his advice on plasmids assembly. This work was supported by grants from ANPCyT/FONCYT (PICT2007-00539) and CONICET (PIP 112 200801 02920/2009–2012). M.S.V., G.C.G. and L.M.E.F. are investigators of the Consejo Nacional de Investigaciones Científicas y Técnicas (CONICET, Argentina).

References

[1] Bhatia S, Tykodi SS, Thompson JA. Treatment of metastatic melanoma: an overview. Oncology (Williston Park) 2009;23:488–96.
[2] Chapman PB, Hauschild A, Robert C, Haanen JB, Ascierto P, Larkin J, et al. Improved survival with vemurafenib in melanoma with BRAF V600E mutation. N Engl J Med 2011;364:2507–16.
[3] Flaherty KT, Infante JR, Daud A, Gonzalez R, Kefford RF, Sosman J, et al. Combined BRAF and MEK inhibition in melanoma with BRAF V600 mutations. N Engl J Med 2012;367:1694–703.
[4] Robert C, Thomas L, Bondarenko I, O'Day S, Weber J, Garbe C, et al. Ipilimumab plus dacarbazine for previously untreated metastatic melanoma. N Engl J Med 2011;364:2517–26.
[5] Ramos-Vara JA, Beissenherz ME, Miller MA, Johnson GC, Pace LW, Fard A, et al. Retrospective study of 338 canine oral melanomas with clinical, histologic, and immunohistochemical review of 129 cases. Vet Pathol 2000;37:597–608.
[6] Smith SH, Goldschmidt MH, McManus PM. A comparative review of melanocytic neoplasms. Vet Pathol 2002;39:651–78.
[7] Finocchiaro LME, Glikin GC. Cytokine-enhanced vaccine and suicide gene therapy as surgery adjuvant treatments for spontaneous canine melanoma. Gene Ther 2008;15:267–76.
[8] Finocchiaro LME, Glikin GC. Cytokine-enhanced vaccine and suicide gene therapy as surgery adjuvant treatments for spontaneous canine melanoma: 9 years of follow-up. Cancer Gene Ther 2012;19:852–61.
[9] Finocchiaro LME, Fiszman GL, Karara AL, Glikin GC. Suicide gene and cytokines combined non viral gene therapy for canine spontaneous melanoma. Cancer Gene Ther 2008;15:165–72.
[10] Gil Cardeza ML, Villaverde MS, Fiszman GL, Altamirano NA, Cwirenbaum RA, Glikin GC, et al. Suicide gene therapy on spontaneous canine melanoma: correlations between in vivo tumors and the corresponding derived in vitro multicellular spheroids. Gene Ther 2010;17:26–36.
[11] Moher D, Hopewell S, Schulz KF, Montori V, Gøtzsche PC, Devereaux PJ, et al. CONSORT 2010 explanation and elaboration: updated guidelines for reporting parallel group randomised trials. BMJ 2010;340:c869.
[12] Chalmers D, Ferrand C, Apperley JF, Melo JV, Ebeling S, Newton I, et al. Elimination of the truncated message from the herpes simplex virus thymidine kinase suicide gene. Mol Ther 2001;4:146–8.
[13] Black ME, Kokoris MS, Sabo P. Herpes simplex virus-1 thymidine kinase mutants created by semi-random sequence mutagenesis improve prodrug-mediated tumor cell killing. Cancer Res 2001;61:3022–6.
[14] Preuss E, Muik A, Weber K, Otte J, von Laer D, Fehse B. Cancer suicide gene therapy with TK.007: superior killing efficiency and bystander effect. J Mol Med (Berl) 2011;89:1113–24.

[15] Yao H, Ng SS, Huo LF, Chow BK, Shen Z, Yang M, et al. Effective melanoma immunotherapy with interleukin-2 delivered by a novel polymeric nanoparticle. Mol Cancer Ther 2011;10:1082–92.
[16] Wiewrodt R, Amin K, Kiefer M, Jovanovic VP, Kapoor V, Force S, et al. Adenovirus-mediated gene transfer of enhanced Herpes simplex virus thymidine kinase mutants improves prodrug-mediated tumor cell killing. Cancer Gene Ther 2003;10:353–64.
[17] Abate-Daga D, Andreu N, Camacho-Sánchez J, Alemany R, Herance R, Millán O, et al. Oncolytic adenoviruses armed with thymidine kinase can be traced by PET imaging and show potent antitumoural effects by ganciclovir dosing. PLoS One 2011;6:e26142.
[18] Choi IK, Yun CO. Recent developments in oncolytic adenovirus-based immunotherapeutic agents for use against metastatic cancers. Cancer Gene Ther 2013;20:70–6.
[19] Han S, Zhang C, Li Q, Dong J, Liu Y, Huang Y, et al. Tumour-infiltrating CD4(+) and CD8(+) lymphocytes as predictors of clinical outcome in glioma. Br J Cancer 2014;13(110):2560–8.
[20] Mac Keon S, Gazzaniga S, Mallerman J, Bravo AI, Mordoh J, Wainstok R. Vaccination with dendritic cells charged with apoptotic/necrotic B16 melanoma induces the formation of subcutaneous lymphoid tissue. Vaccine 2010;28:8162–8.
[21] Dieu-Nosjean MC, Antoine M, Danel C, Heudes D, Wislez M, Poulot V, et al. Long term survival for patients with non-small-cell lung cancer with intratumoral lymphoid structures. J Clin Oncol 2008;26:4410–7.
[22] Wiggans MG, Shahtahmassebi G, Malcolm P, McCormick F, Aroori S, Bowles MJ, et al. Extended pathology reporting of resection specimens of colorectal liver metastases: the significance of a tumour pseudocapsule. HPB (Oxford) 2013;15:687–94.
[23] Okano K, Yamamoto J, Kosuge T, Yamamoto S, Sakamoto M, Nakanishi Y, et al. Fibrous pseudocapsule of metastatic liver tumors from colorectal carcinoma. Clinicopathologic study of 152 first resection cases. Cancer 2000;89:267–75.
[24] Miura Y, Suda A, Watanabe Y, Yamakawa M, Imai Y. Inflammatory cells in the pseudocapsule of osteosarcoma. A clinicopathologic analysis. Clin Orthop Relat Res 1994;300:225–32.
[25] O'Donnell PW, Manivel JC, Cheng EY, Clohisy DR. Chemotherapy influences the pseudocapsule composition in soft tissue sarcomas. Clin Orthop Relat Res 2014;472:849–55.
[26] Gitelis S, Thomas R, Templeton A, Schajowicz F. Characterization of the pseudocapsule of soft-tissue sarcomas. An experimental study in rats. Clin Orthop Relat Res 1989;246:285–92.
[27] Li S, Wilkinson M, Xia X, David M, Xu L, Purkel-Sutton A, et al. Induction of IFN-regulated factors and antitumoral surveillance by transfected placebo plasmid DNA. Mol Ther 2005;11:112–9.
[28] Roman M, Martin-Orozco E, Goodman JS, Nguyen MD, Sato Y, Ronaghy A, et al. Immunostimulatory DNA sequences function as T helper-1-promoting adjuvants. Nat Med 1997;3:849–54.
[29] Shu CJ, Guo S, Kim YJ, Shelly SM, Nijagal A, Ray P, et al. Visualization of a primary anti-tumor immune response by positron emission tomography. Proc Natl Acad Sci U S A 2005;102:17412–7.
[30] Laing RE, Nair-Gill E, Witte ON, Radu CG. Visualizing cancer and immune cell function with metabolic positron emission tomography. Curr Opin Genet Dev 2010;20:100–5.
[31] Dunn GP, Bruce AT, Ikeda H, Old LJ, Schreiber RD. Cancer immunoediting: from immunosurveillance to tumor escape. Nat Immunol 2002;3:991–8.
[32] Schreiber RD, Old LJ, Smyth MJ. Cancer immunoediting: integrating immunity's roles in cancer suppression and promotion. Science 2011;331:1565–70.
[33] Huang B, Pan PY, Li Q, Sato AI, Levy DE, Bromberg J, et al. Gr-1^{+}CD115^{+} immature myeloid suppressor cells mediate the development of tumor-induced T regulatory cells and T-cell anergy in tumor-bearing host. Cancer Res 2006;66:1123–31.
[34] Kornete M, Piccirillo CA. Functional crosstalk between dendritic cells and Foxp3(+) regulatory T cells in the maintenance of immune tolerance. Front Immunol 2012;3:165.
[35] Strauss L, Bergmann C, Szczepanski MJ, Lang S, Kirkwood JM, Whiteside TL. Expression of ICOS on human melanoma-infiltrating CD4 + CD25highFoxp3 + T regulatory cells: implications and impact on tumor-mediated immune suppression. J Immunol 2008;80:2967–80.
[36] Allan SE, Crome SQ, Crellin NK, Passerini L, Steiner TS, Bacchetta R, et al. Activation-induced FoxP3 in human T effector cells does not suppress proliferation or cytokine production. Int Immunol 2007;19:345–54.
[37] Hamid O, Schmidt H, Nissan A, Ridolfi L, Aamdal S, Hansson J, et al. A prospective phase II trial exploring the association between tumor microenvironment biomarkers and clinical activity of ipilimumab in advanced melanoma. J Transl Med 2011;9:204.
[38] Lladser A, Mougiakakos D, Tufvesson H, Ligtenberg MA, Quest AF, Kiessling R, et al. DAI (DLM-1/ZBP1) as a genetic adjuvant for DNA vaccines that promotes effective antitumor CTL immunity. Mol Ther 2011;19:594–601.
[39] Veterinary Co-operative Oncology Group. Common Terminology Criteria for Adverse Events (VCOG-CTCAE) following chemotherapy or biological antineoplastic therapy in dogs and cats v1.0. Vet Comp Oncol 2004;2:195–213.